Electrochemically Assisted Persulfate Oxidation of Organic Pollutants in Aqueous Solution: Influences, Mechanisms and Feasibility

Jianting Sun [1], **Wei Zheng** [1], **Gang Hu** [1], **Fan Liu** [1], **Siyuan Liu** [1], **Lie Yang** [2,*] and **Zulin Zhang** [2,3,*]

[1] Wuhan Huantou Qianzishan Environmental Industry Co., Ltd., Wuhan 430000, China
[2] School of Resources and Environmental Engineering, Wuhan University of Technology, Wuhan 430070, China
[3] The James Hutton Institute, Craigiebuckler, Aberdeen ABI5 8QH, UK
[*] Correspondence: yanglie612@whut.edu.cn (L.Y.); zulin.zhang@hutton.ac.uk (Z.Z.)

Abstract: Electrochemically (EC) assisted persulfate (PS) oxidation processes (EPOPs) have gained increasing attention in recent years. In this review, the current status and prospects of EC/PS degradation of organic pollutants are discussed and summarized. It was found that the oxidation of most organic contaminants could be significantly enhanced or accelerated using the combination of EC and PS compared to single treatments. Moreover, the effects of various operational variables on the removal of organic contaminants were investigated. Some variables are highly sensitive, and the optimal conditions are case-specific. Regarding the degradation mechanisms, radical-induced reactions and nonradical reactions both exist for the elimination of organic contaminants. Oxidants (including $S_2O_8^{2-}$ and $SO_4^{\bullet-}$) can be produced from SO_4^{2-} near the anode, which is a unique feature of EPOPs. In some studies, the electrical energy consumption of EPOPs has been controlled to a reasonably low level in lab-scale attempts. Although there are still a few drawbacks or difficulties (e.g., potential electrode fouling, dependency on batch mode) for large-scale applications, EPOPs offer a promising alternative to traditional advanced oxidation techniques.

1. Introduction

Hydrogen peroxide (H_2O_2) is a typical oxidant in traditional advanced oxidation processes. In recent years, persulfate (PS, including permonosulfate (PMS) and peroxodisulfate (PDS)) has gained great interest as a promising alternative to H_2O_2 for advanced oxidation processes due to its high redox potential and longer lifetime [1–3]. Although the price of PS (e.g., ammonium persulfate, USD 715–USD 815 per ton) is higher than that of H_2O_2 (USD 470–USD 610 per ton) (https://www.alibaba.com/, accessed on 1 November 2022), PS can be easily stored and delivered in a solid form due to its stability in the inactive state [1,4]. In addition, the chemical cost was reported to be much lower than the energy cost for the treatment of some refractory organic pollutants (e.g., per- and polyfluoroalkyl substances) [5]. In view of standard electrode potentials, $SO_4^{\bullet-}$ (E^0 = 2.5V~3.1 V) can be formed when the O-O bonds in PS (E^0 = 2.1 V) are broken using various activation methods [2,6]. Traditional $^{\bullet}OH$ radicals have a standard reduction potential of 2.7 V in an acidic solution and 1.8 V in a neutral solution [7]. Several activation methods have been explored in the past decade, including energy input (e.g., heat [8,9], ultrasound [2], ultraviolet rays [10], electrochemistry [11], and microwave [12]), nano-materials [13], transition metals [14,15], and carbon materials [16]. Among these techniques, electrochemical activation is an emerging choice and has attracted increasing attention during the past 12 years (Figure 1) based on statistical data from the Web of Science (www.webofscience.com, accessed on 1 November 2022). Electrochemical oxidation technology can be utilized alone for the decomposition of organic pollutants, e.g., ciprofloxacin [17], enrofloxacin [18], and perfluorooctane sulfonate [19].
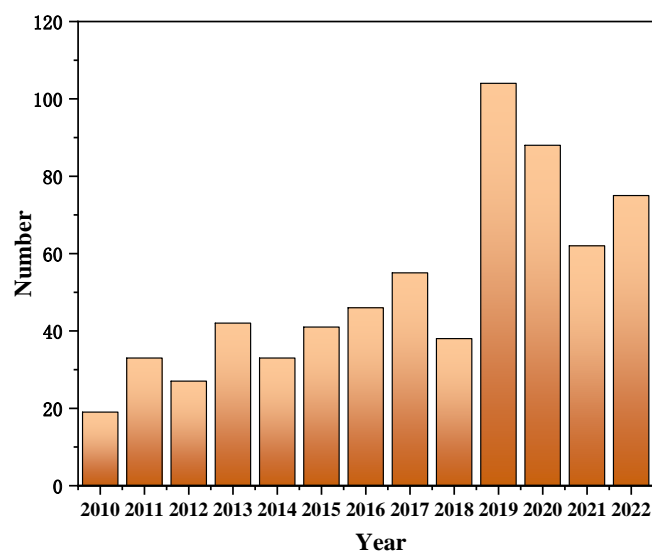
Figure 1. The output of research publications using the EC-PS degradation system by the end of 2022. Searched terms: "electrochemistry" and "persulfate". Source: Web of Science (December 2022).

It was reported that at various Fe^{2+} dosages (2 mg/L, 4 mg/L, 6 mg/L and 8 mg/L), the phenol degradation and COD removal observed were much higher in electro-Fenton processes than in traditional Fenton processes [20]. In particular, electro-Fenton processes could be significantly enhanced when PS was added [21]. The addition of PS can provide sufficient oxidants and facilitate the degradation of organic contaminants [22]. The combination between electrochemistry (EC) and PS is a promising substitution for traditional advanced oxidation processes. On the one hand, electron transfer from the electrochemical process can activate PS to generate $SO_4^{\bullet-}$ [23]. The values of the standard one-electron reduction potentials of $SO_4^{\bullet-}$ and $S_2O_8^{2-}$ are 2.437 +/− 0.019 and 1.44 +/− 0.08 V vs. the standard hydrogen electrode (SHE), respectively [24]. $SO_4^{\bullet-}$ could attack target compounds and generate byproducts including SO_4^{2-} [8,9]. On the other hand, $S_2O_8^{2-}$ can be generated from SO_4^{2-} on the surface of an anode [25–27]. The regeneration process of $S_2O_8^{2-}$ can provide an effective supply of oxidants. Compared to other PS activation methods, this unique feature of electro-activated PS is beneficial for cost reduction in further full-scale applications, which could explain why the electrochemical activation method has gained increasing interest.

A number of attempts have been made to eliminate various organic pollutants using EC-assisted PS-based oxidation processes (EPOPs), including dyes [23,28], pharmaceuticals [29,30], and herbicides [31], among others. The performance of EPOPs in these studies was not the same, mainly due to the different operational variables and degradation mechanisms. Thus, a detailed review is necessary to outline and discuss the current status and trends in EPOPs. Although several reviews on electrochemical advanced oxidation processes (EAOPs) were reported in recent years [32–35], these reviews mainly focused on H_2O_2-based processes. Li et al. [36] conducted a mini-review involving EAOPs–PS systems and EAOPs–PMS systems, which primarily discussed the reaction mechanisms of homogeneous (Fe^{2+} and Fe^{3+}) and heterogeneous catalysts (Fe, Mn, and Co oxides) [36]. Nevertheless, the radical and non-radical mechanisms of organic pollutant degradation in EPOPs have not been systematically summarized yet. The conversion between $S_2O_8^{2-}$ and SO_4^{2-} was not discussed in the previous review. In addition, the synergistic influences of EC and PS and operational variables in EPOPs were not reviewed yet. Therefore, this review places emphasis on the following targets: (1) to summarize the synergistic influences of EC and PS on the removal of organic contaminants; (2) to discuss the influences of operational variables on organic contaminant removal; (3) to analyze and outline the predominant degradation mechanisms of EPOPs; and (4) to investigate the energy consumption of EPOPs.

2. Synergistic Influences of EC and PS

Electrochemical oxidation technology can be utilized alone for the decomposition of organic pollutants [17–19]. Electrochemical oxidation of contaminants occurs through two reaction paths including direct anodic oxidation and indirect oxidation [37,38]. Both mechanisms involve electron transfer, which can be used to activate PS [23]. In view of the promising combination of EC and PS, the performances of single and combined EC and PS treatments are compared to analyze their synergistic effects on the decomposition of various pollutants (Table 1). It is worth mentioning that significant differences are observed in the outcome of these methods for the removal of various organic contaminants, probably due to the differences in operational variables and molecular structures. The degradation efficiencies of the "EC + PS" combination are better than those of single EC or PS oxidation processes for most of the selected target compounds. Moreover, single EC is more efficient for the majority of selected organic pollutants than sole PS treatment. Unactivated PS was ineffective during the degradation processes probably due to its lower redox potential ($S_2O_8^{2-}$, E^0 = 2.1 V) than that of $SO_4^{\bullet-}$ (E^0 = 2.5 V~3.1 V) [23,28,29]. Single electrochemical oxidation was also found to be inefficient for several target compounds, e.g., bisphenol A [29] and carbamazepine [39] with 3.5% and 2.18% removal efficiencies, respectively. Once the two methods are combined, significant enhancement can be achieved for bisphenol A and carbamazepine with 76.5% and 97.76% removal efficiencies, respectively. It was found that the concentrations of diuron remained unchanged when treated with PS alone, and only 15% of diuron was removed with EC treatment [40]. Nevertheless, over 77% of diuron was eliminated when the EC/PS system was employed [40]. Analogously, negligible oxcarbazepine (OXC) was degraded using PS alone and a similar low removal was obtained with the application of electrocoagulation alone [30]. In contrast, a high removal rate of ~75% was achieved within only 10 min when 0.5 mM PS was added [30]. On the whole, the combination of EC and PS is a promising advanced oxidation system for aqueous refractory organic contaminants and trace contaminants.

Table 1. Synergistic effects of EC and PS on organic contaminant removal.

System	Analytes	Analyte Conc.	Removal Efficiency (%/min)			Ref.
			PS/Contact Time	EC/Contact Time	EC + PS/Contact Time	
Fe-C/PS	2,4-dinitrotoluene	100 mg/L	≈20/340	-	94/340	[41]
EC/Fe^{2+}/PDS	Acid Orange 7	0.1 mM	0/60	65.8/60	71.6/60	[23]
EC/Catalyst/PDS	Acid Orange 7	0.14 mM	67.4/30	-	67.4/30	[42]
EC/PDS	Aniline	60 mg/L	18/420	21/420	55/420	[43]
EC/US/PDS	Aniline	75 mg/L	22/420	-	69/420	[44]
EC/PDS	Aniline	0.45 mM	20/150	-	98/150	[45]
EC/PDS	Atrazine	5 μM	0/30	36.3/30	78.2/30	[31]
EC/PDS	Atrazine	2 μM	<10/20	-	90.6/10	[46]
EC/Fe^{3+}/PDS	Bisphenol A	0.22 mM	0/60	0/60	26.3/60	[29]
EC/Catalyst/PDS	Bisphenol A	0.1 mM	4.1/60	1.8/60	7.6/60	[47]
EC/Catalyst/PMS	Bisphenol A	50 μM	0/80	8/80	41.6/80	[48]
EC/PDS	Carbamazepine	5 μM	9/30	82/30	88/20	[49]
EC/PDS	Carbamazepine	5 μM	-	65/60	81/30	[50]
EC/Fe^{3+}/PMS	Carbamazepine	0.04mM	1.9/30	2.18/30	12.68/30	[39]
EC/PDS	Carbamazepine	0.042 mM	6.87/30	43.04/30	98.78/30	[51]
EC/PDS	Ciprofloxacin	30 mg/L	0/80	≈40/80	96/80	[52]
EC/PDS	Ciprofloxacin	20 mg/L	0/160	25/160	90.37/160	[53]
EC/PDS	Diuron	10 μM	0/15	15/15	77/15	[40]
EC/PDS	Dinitrotoluenes	300 mg/L (TOC)	4/480	45/480	70/480	[54]
EC/Catalyst/PDS	Orange II	100 mg/L	0/60	89.4/60	91.2/60	[28]
EC/PDS	Oxcarbazepine	20 μM	<1/10	9/10	75/10	[30]
EC/FeCl$_2$/PDS	Phenol	100 mg/L	0/60	-	<5/60	[55]
EC/PDS	Sulfamethoxazole	5 μM	-	58/30	96/30	[56]
EC/PDS	Tetracycline hydrochloride	50 mg/L	19.8/240	43.8/240	≈81/240	[57]

3. Influence of Operational Parameters on the Degradation Efficiency of EPOPs

3.1. Electrode Material

The electrode material is one of the most vital factors determining the efficiency and cost of the electrochemical process [58]. The electrocatalytic activity, service life, and stability are the most important characteristics of the anode/cathode materials [58]. There has been increasing concern for electrode materials in EPOPs [36]. The commonly used electrodes include anode materials such as mixed metal oxides (e.g., Ti/RuO_2-IrO_2) [23,29,59], iron sheet [42,60,61], carbon felt [62], cathode with titanium [63], stainless steel [55], and carbon fiber [64]. Some electrode materials do not react with electrolytes, while several materials (e.g., iron) participate in the redox reactions in EPOPs [60]. It is known that Fe^{2+} is a typical activator of PDS and PMS via Equations (1) and (2) [36,65]. The generated Fe^{3+} can be reduced to Fe^{2+} by the cathodic reaction (Equation (3)) [66], and then Fe^{2+} can activate PS in the solution again. Therefore, Fe^{2+} has been frequently applied to enhance the degradation efficiency of EPOPs due to its outstanding ability to activate PS [23,55,67,68]. However, excessive Fe^{2+} can simultaneously scavenge sulfate radicals via Equation (4) [66], which would undoubtedly reduce the oxidation efficiency. In particular, the iron electrode could be used to control the release of Fe^{2+} via the anodic reaction (Equation (5)) to optimize the degradation process, as reported in previous studies [66,69]. Moreover, the effective current transfer between the anode and cathode would probably be reduced by the formation of a hydrated iron hydroxide/oxide film on the surface of the iron anode. This problem could be avoided by using an acidic pH condition. The positive effect of acidic pH will be discussed in Section 3.4 in more detail.

$$Fe^{2+} + S_2O_8{}^{2-} \rightarrow Fe^{3+} + SO_4{}^{2-} + SO_4{}^{\bullet-} \tag{1}$$

$$Fe^{2+} + HSO_5{}^- \rightarrow Fe^{3+} + OH^- + SO_4{}^{\bullet-} \tag{2}$$

$$Fe^{3+} + e^- \rightarrow Fe^{2+} \tag{3}$$

$$Fe^{2+} + SO_4{}^{\bullet-} \rightarrow Fe^{3+} + SO_4{}^{2-} \tag{4}$$

$$Fe(s) \rightarrow Fe^{2+} + 2e^- \tag{5}$$
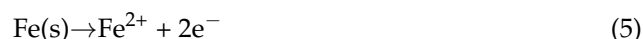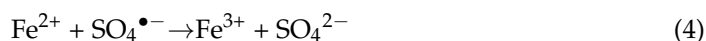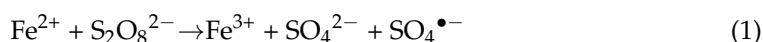
In addition to the iron electrode, there are also significant differences in the degradation efficiency among non-active electrodes. It was found that ampicillin removal rates after 10 min of reaction were 68% and 39% for boron-doped diamond (BDD) and platinum anodes, respectively [70]. The strong contact of hydroxyl radicals on the surface and the lower potential window of platinum were considered to be the main reasons for the observed phenomenon [70]. Furthermore, the oxygen evolution overpotential of electrode materials is believed to be vital for the oxidation of organic contaminants [37]. Therefore, high O_2 overvoltage anodes such as BDD are usually preferred [37]. Cathode materials are also important for analyte removal in EPOPs. The removal of ciprofloxacin and total organic carbon was compared between BDD/Pt and BDD/Gr electrode pairs in a single-cell rotating disk electrode system to evaluate how cathode materials affect EPOPs during analyte removal [71]. The results indicated that ciprofloxacin and total organic carbon (TOC) degradation rates were statistically insignificant with Pt- and Gr-cathodes, and graphite was a suitable substitute for platinum [71]. During the PS activation process, the concentration of sulfate ions would inevitably increase. Some of the sulfate ions could be converted to PS again [25]. Nonetheless, the final concentration of sulfate ions in the effluent was not investigated in previous studies.

3.2. Electrolyte Type and Concentration

An electrolyte is the medium of electrochemical reactions, which can provide the precursors of reactive oxidizing species [71,72]. A suitable electrolyte is necessary for the efficient removal of organic pollutants in EPOPs. The effects of nitrate, sulfate, and persulfate electrolytes on ciprofloxacin removal in an electrochemical reactor were compared [71].

Ciprofloxacin was efficiently removed with EC/PS treatment, achieving 84% after 120 min and reaching 90% after 240 min [71]. The removal rate in sulfate was slower, although a similar degree of removal was achieved within 240 min [71]. Nevertheless, a much slower removal of ciprofloxacin was observed when nitrate was employed as the electrolyte, reaching 90% in 24 h [71]. Cathodic persulfate activation occurred when persulfate was added as the electrolyte, and $SO_4^{\bullet-}$ could attack ciprofloxacin effectively [71]. Moreover, $S_2O_8^{2-}$ could be generated from SO_4^{2-} via Equation (6) [26,27,73,74]. The electrochemical oxidation of multiple organic compounds was also studied while varying the background electrolyte among NaCl, Na_2SO_4, and NaClO4 [75]. When the electrolyte exchanged from ClO_4^- to Cl^- or SO_4^{2-}, the anodic oxidation performance became substrate-specific, probably because the electrolyte-derived reactive species ($Cl_2^{\bullet-}$, $SO_4^{\bullet-}$) contributed to the overall electrochemical oxidation efficiency [75]. Overall, Cl^- and SO_4^{2-} acted as the precursors of reactive oxidizing species ($Cl_2^{\bullet-}$, $SO_4^{\bullet-}$) and contributed to the organic decomposition in EPOPs, while ClO_4^- and NO_3^- could only depend on anode oxidation.

$$2SO_4^{2-} \rightarrow S_2O_8^{2-} + 2e^- \tag{6}$$

Apart from the electrolyte type, the electrolyte concentration is another major concern for the medium optimization. There are several studies focusing on the influence of electrolyte concentration on the degradation of organic contaminants [29,39,74]. It is well known that conductivity increases with an increase in electrolyte concentration. Nevertheless, the relationship between electrolyte concentration and the degradation of organic contaminants is much more complicated. As previously mentioned, ClO_4^- and NO_3^- can only depend on anode oxidation via $^{\bullet}OH$ reactions. It was observed that the reaction rates marginally improved over the range of 0.75 h^{-1} to 1.06 h^{-1} with 8.5–60 mM $NaNO_3$ [74]. Regarding Na_2SO_4, it was found that the decomposition rate of bisphenol A decreased when the concentration increased from 50 to 200 mM [29], probably due to the voltage decline of the system [39]. A similar phenomenon was observed in the degradation of carbamazepine in EPOPs. It is worth mentioning that a sufficient amount of SO_4^{2-} is necessary for efficient oxidation in EPOPs. The concentration of 40 mM was determined to be optimal when the Na_2SO_4 concentration was varied from 5 mM to 40 mM [74]. Therefore, electrochemical oxidation is substrate-specific when an electrolyte is the precursor of reactive oxidizing species, and an appropriate electrolyte concentration is vital for the efficient degradation of organic contaminants.

3.3. Current Density

Current density (CD) has been frequently investigated for optimizing the electrochemical oxidation processes [23,28,29]. Previous studies involving CD optimization are presented in Table 2. On the one hand, a higher current density improved the generation of sulfate radicals via an electron transfer reaction [29]. On the other hand, increasing the CD led to faster ferrous ion production and regeneration rate when an iron anode, Fe^{2+}, and Fe^{3+} were used [29,39]. In addition, $S_2O_8^{2-}$ can be generated from SO_4^{2-} in the electrolyte via Equation (6), as mentioned above [25]. It was found that a significant increase in the production of $S_2O_8^{2-}$ was achieved at 30 mA·cm^{-2} and 60 mA·cm^{-2}, compared to that at 15 mA·cm^{-2} [25]. This process could be considered as the in situ generation of oxidant supply. Nevertheless, it was also observed that there was no enhancement in the pollutant degradation when further increasing the CD after it reached a limit [39,76]. The limit depended on the target contaminants. When the current density reached the limit, the inhibition effect on pollutant removal became significant. Han et al. [39] found that the removal rate of carbamazepine was increased as the CD was switched from 3.57 to 7.14 mA/cm^2. Nonetheless, no significant improvement was observed when the CD increased from 7.14 to 14.28 mA/cm^2 [39]. Similarly, the COD removal from landfill leachate using oxidation, as well as the total COD removal, increased significantly as the CD increased from 40 mA to 80 mA, while a further increase in the current did not lead to a clear improvement in COD removal [76]. This phenomenon could be attributed to some side reactions such as

hydrogen evolution (Equation (7)) and PDS reduction (Equation (8)). In addition, it was noticed that the optimal current densities of some compounds (e.g., phenol and ciprofloxacin) reported in different publications were significantly different. For most entries, higher current densities could achieve higher removal rates of organic pollutants. The main reason for this phenomenon was the different range of the selected current density. These target pollutants were degraded with higher removal rates under higher current densities.

$$2H^+ + 2e^- \rightarrow H_2 \tag{7}$$

$$S_2O_8{}^{2-} + 2e^- \rightarrow 2SO_4{}^{2-} \tag{8}$$

Table 2. Effects of current density on degradation efficiencies of organic contaminants in EPOPs.

Analytes	Selected Current Densities	Optimal Current for Higher Removal Rates	Ref.
1-Butyl-1-methylpyrrolidinium chloride	25, 50, 100, 150 mA	150 mA	[77]
2,4,6-Trichlorophenol	50, 60, 70, 80, 90 mA	90 mA	[78]
2, 4-Dinitrophenol	2, 4, 6, 8, 10 mA·cm^{-2}	4 mA·cm^{-2}	[79]
Acid Orange 7	8.4, 16.8, 33.6 mA·cm^{-2}	33.6 mA·cm^{-2}	[23]
Acid Orange 7	2, 4, 12, 16 mA·cm^{-2}	16 mA·cm^{-2}	[42]
Ampicillin	5, 10, 25, 110 mA·cm^{-2}	110 mA·cm^{-2}	[70]
Atrazine	1, 3, 5, 7, 9 mA·cm^{-2}	9 mA·cm^{-2}	[31]
Atrazine	4, 8, 12, 16, 20, 24 mA·cm^{-2}	24 mA·cm^{-2}	[80]
Basic Red 18	100, 200, 300, 400 mA	400 mA	[81]
Bisphenol A	1.68, 3.36, 5.04, 8.40 mA·cm^{-2}	8.40 mA·cm^{-2}	[47]
Bisphenol A	8.4, 16.8, 33.6 mA·cm^{-2}	33.6 mA·cm^{-2}	[29]
Bisphenol A	50, 100, 150 mA·m^{-2}	150 mA·m^{-2}	[48]
Carbamazepine	0.1×10^5, 0.5×10^5, 1×10^5, 2×10^5 mA·m^{-2}	2×10^5 mA·m^{-2}	[50]
Carbamazepine	3.57, 7.14, 10.71, 14.28 mA·cm^{-2}	14.28 mA·cm^{-2}	[39]
Ciprofloxacin	0.75, 1.45, 2.3 mA·cm^{-2}	1.45 mA·cm^{-2}	[52]
Ciprofloxacin	0.9, 1.55, 2.75, 4.25 mA·cm^{-2}	2.75 mA·cm^{-2}	[53]
Cu-EDTA	0.1, 0.2, 0.5, 1.0 mA·cm^{-2}	1.0 mA·cm^{-2}	[82]
Diatrizoate	1×10^5, 1.5×10^5, 2×10^5 mA·m^{-2}	2×10^5 mA·m^{-2}	[74]
Disperse Blue 3	5, 10, 20, 30, 40, 80 mA·cm^{-2}	80 mA·cm^{-2}	[83]
Diuron	10, 20, 30, 40 mA	40 mA	[40]
Hexachlorocyclohexanes	0, 10, 20 mA	20 mA	[84]
Orange II	5.0, 8.4, 11.8, 16.8 mA·cm^{-2}	16.8 mA·cm^{-2}	[85]
Orange II	1.68, 5.04, 8.40, 11.76, 16.80 mA·cm^{-2}	16.8 mA·cm^{-2}	[28]
Oxcarbazepine	1.6–50.0 mA·cm^{-2}	8.3 mA·cm^{-2}	[30]
Phenol	1, 3, 5, 10 mA·cm^{-2}	10 mA·cm^{-2}	[61]
Phenol	140, 270, 540 mA·L^{-1}	540 mA·L^{-1}	[60]
Phenol	20, 40, 80, 120 mA·cm^{-2}	120 mA·cm^{-2}	[86]
Pentachlorophenol	15, 30, 45, 60, 75, 90 mA	90 mA	[87]
Reactive Brilliant Blue	5, 7.5, 10, 20 mA·cm^{-2}	20 mA·cm^{-2}	[88]
Sulfamethoxazole	10, 50, 100, 200 A·m^{-2}	200 A·m^{-2}	[56]
Sulfamethoxazole	5, 10, 15, 20 mA	20 mA	[89]
Tetracycline hydrochloride	6.67, 10, 13.33, 16.67 mA·cm^{-2}	13.33 mA·cm^{-2}	[57]
Trichloroethylene	−50, −25, −10, 0, 25, 50, 100 mA	100 mA	[90]

Inhibition effects on the removal of organic pollutants were found with further increases in the CD [30,53,81]. The removal rate of oxcarbazepine decreased rapidly when the CD increased over 8.3 mA/cm^2, which can be attributed to the quenching of $^\bullet$OH

and $SO_4^{\bullet-}$ due to the excess Fe^{2+} produced from the anode [30]. Analogously, the ciprofloxacin removal rates at the contact time of 40 min and a CD of 0.94, 1.55, 1.75, 2.75, and 4.25 mA/cm^2 were 79.65, 87.55, 89.32, and 80.31%, respectively [53]. It was obvious that the CIP removal efficiency decreased with the increase in CD to 4.25 mA/cm^2 [53]. A similar phenomenon was observed in a study of Basic Red 18 decolorization using EPOPs [81]. On the whole, increasing the current density could promote the degradation of organic contaminants within an appropriate limit. Further increases would inhibit the oxidation processes probably due to hydrogen evolution, PDS reduction, and excess Fe^{2+} generation.

3.4. Initial pH

The initial pH plays an important role in the degradation of contaminants in $SO_4^{\bullet-}$-grounded systems [2,91]. The influences of pH on the removal efficiencies in EPOPs have been frequently investigated (Table 3). Most of the previous studies found that an acidic pH was favorable for the degradation of selected organic contaminants in EPOPs. The phenomenon was attributed to the notable decline in soluble oxygen gas in wastewater at low pH values, which could facilitate the contact between persulfate anions and the cathode and result in the formation of sulfate radicals [43,44]. Moreover, when the reaction occurred in the presence of Fe^{2+} or Fe^{3+}, a Fe-containing precipitate was generated to retard the oxidation process [29]. When the pH was greater than 4.0, ferric ions formed some Fe^{3+} oxyhydroxides, such as $FeOH^{2+}$, $Fe_2(OH)_2^{4+}$, $Fe(OH)^{2+}$, and $Fe(OH)_3$ (Equations (9) and (10)) [29,92]. A similar phenomenon was observed in the presence of Fe^{2+} via Equation (11) [29,39]. The precipitate formation is believed to inhibit the activation reaction between Fe^{2+} and PDS [29]. In addition, $SO_4^{\bullet-}$ can react with OH^- to generate $^{\bullet}OH$ (a weaker oxidant) via Equation (12) under alkaline conditions [2].

$$Fe^{3+} + H_2O \rightarrow FeOH^{2+} + H^+ \tag{9}$$

$$2Fe^{3+} + 2H_2O \rightarrow Fe_2(OH)_2^{4+} + 2H^+ \tag{10}$$

$$Fe^{2+} + H_2O \rightarrow FeOH^+ + H^+ \tag{11}$$

$$SO_4^{\bullet-} + OH^- \rightarrow SO_4^{2-} + HO^{\bullet} \tag{12}$$
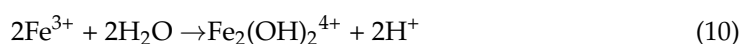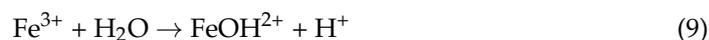
Nonetheless, a low pH is not always favorable for the oxidation of organic contaminants. When the initial pH of Orange II decreased from 3 to 2, the initial decolorization rate and efficiency decreased slightly [28]. Similarly, a further decrease in pH from 4.00 to 2.00 caused a significant drop in the degradation of tetracycline hydrochloride [57]. A high H^+ concentration would promote the side reaction of H_2 generation via Equation (7). In particular, it was found that the rate constant was significantly increased under acidic (pH = 3) and alkaline conditions (pH = 12) [83]. Therefore, it could be deduced that alkaline activation plays a vital role in the initial stage when the initial pH is set at 12. In addition, pH_{PZC} of the applied catalysts could be relevant to optimal pH when a catalyst is combined with the EC/PS processes [42,51,80]. Moreover, a pH adjustment for efficient removal contributes to the operational cost of EPOPs. Overall, the optimal pH in EPOPs depends on a series of factors including the soluble oxygen, Fe^{2+}/Fe^{3+}, and catalyst.

Table 3. Investigations of optimal pH values in EPOPs.

Analytes	Selected pH Values	Optimal Ph For Higher Removal Rates	Ref.
2, 4-Dinitrophenol	3, 4, 5, 7, 8, 9, 11	3	[79]
2,4,6-Trichlorophenol	3, 5, 7, 9, 11	9	[78]
2,4-dinitrotoluene	2, 3, 5, 7, 9, 11	2	[41]
Acid Orange 7	3, 7, 9	3	[23]
Acid Orange 7	3, 6, 9, 11	3	[42]
Aniline	3, 4, 5, 7	3	[43]
Aniline	3, 4, 5, 7	3	[44]
Atrazine	4, 6, 8, 10	4	[31]
Atrazine	3, 5, 6.3, 7, 9, 11	3	[80]
Bisphenol A	3, 6, 9	3	[29]
Bisphenol A	3, 6.6, 9	3	[48]
Carbamazepine	5, 7, 9	5	[51]
Carbamazepine	3, 5, 7, 9, 11	3	[39]
Ciprofloxacin	3, 5, 7, 9	5	[52]
Ciprofloxacin	3, 5, 7, 9	7	[53]
Dinitrotoluenes	0.5, 1, 2, 3	0.5	[54]
Disperse Blue 3	3, 6.3, 9, 12	12	[83]
Diuron	3, 5, 7, 9, 11	3	[40]
Landfill leachate	3.5, 6.5, 8.5, 12	3.5	[93]
Methyl orange	3, 5, 7, 9	3	[69]
Orange II	2, 3, 6, 9	3	[28]
Orange II	3, 6, 7, 9	3	[85]
Oxcarbazepine	3, 5, 7, 9, 11	3	[30]
Pentachlorophenol	4.5, 6.5, 8.5	4.5	[87]
Petrochemical wastewater	3, 5, 7, 9	3	[94]
Ponceau 6R	0.5, 1, 2, 3	2	[95]
Reactive Brilliant Blue	3, 6, 9, 11	6	[88]
Sodium dodecylbenzene sulfonate	3, 6, 7, 9, 11	3	[68]
Sulfamethoxazole	1, 2, 3, 4	3	[89]
Tetracycline hydrochloride	2, 4, 7, 9	4	[57]

3.5. PS Concentration

The effects of the initial PS concentration in EPOPs are summarized in Table 4. As demonstrated in Table 4, the removal rates exhibited a significant increasing trend with the increase in PS concentration in some previous studies [23,28,87]. This phenomenon could be attributed to the significant increase in the number of sulfate radicals [54]. PS is the chief source of sulfate radicals in the system, and more reactive radicals would be generated to degrade the organic contaminants at a higher PS concentration [23]. Some other studies found that when the PS concentration reached a certain limit, a further increase in PS concentration did not promote and even inhibited the degradation efficiency [29,51,85]. It was observed that the TOC removal efficiency exhibited an increasing trend with the addition of persulfate anions in the prepared aniline solution [44]. However, in the presence of excess persulfate anions (3.0 wt%), the removal rate of aniline was decreased [44]. Similar phenomena were found in other studies involving hexachlorocyclohexanes [84], methyl orange [69], sodium dodecylbenzene sulfonate [68], and dinitrotoluenes [96]. The side reactions between $S_2O_8^{2-}$ and reactive radicals (Equations (13) and (14)) could probably explain this phenomenon when excess PS is added, which would consume more $S_2O_8^{2-}$ [29,85]. It is evident that an excess persulfate anion concentration would inhibit the formation of hydrogen peroxide from sulfate radicals [43]. Additionally, the recombination of sulfate radicals (Equation (15)) may also occur under excess PS concentrations [51]. The mentioned side reactions are consistent with other PS-based processes [2]. In particular, it was noted that the optimal PS concentrations of some compounds (e.g., aniline and atrazine) reported in different publications were significantly different. Indeed, the results were consistent with the above analysis. Three atrazine-based studies indicated that the removal rates

increased with the increase in PS concentration. When the range of PS concentrations was extended, excessive PS concentration caused side reactions, thus decreasing the removal efficiency. The limit values are target-dependent and easily affected by the operational conditions. Therefore, the selection of PS concentration should consider the degradation rates and economic costs.

$$S_2O_8{}^{2-} + SO_4{}^{\bullet-} \rightarrow S_2O_8{}^{\bullet-} + SO_4{}^{2-} \tag{13}$$

$$S_2O_8{}^{2-} + {}^{\bullet}OH \rightarrow S_2O_8{}^{\bullet-} + OH^- \tag{14}$$

$$SO_4{}^{\bullet-} + SO_4{}^{\bullet-} \rightarrow S_2O_8{}^{2-} \tag{15}$$

Table 4. Effects of PS concentrations on the degradation efficiencies of organic contaminants in EPOPs.

Analytes	Selected PS Concentrations	Optimal PS Concentration	Ref.
2, 4-dinitrophenol	1, 2, 4, 5, 6, 8 mM	5 mM	[79]
2,4-dinitrotoluene	0.037, 0.185, 0.37, 1.85, 3.7 mM	0.185 mM	[41]
Acid Orange 7	2, 4, 8, 12 mM	12 mM	[23]
Acid Orange 7	2.1, 4.2, 8.4 mM	8.4 mM	[42]
Ampicillin	0.42, 1.05, 2.1 mM	2.1 mM	[70]
Aniline	42, 84, 126, 168 mM	126 mM	[43]
Aniline	42, 84, 105, 126 mM	105 mM	[44]
Aniline	1.85, 3.7, 5.55, 7.4 mM	7.4 mM	[45]
Atrazine	0.25, 0.5, 1, 2, 5 mM	5 mM	[31]
Atrazine	0.3, 0.5, 1, 3, 5 mM	5 mM	[46]
Atrazine	1, 2, 3, 4, 4.5 mM	4.5 mM	[80]
Bisphenol A	1, 5, 10, 20 mM	10 mM	[29]
Bisphenol A	5, 10, 15 mM	15 mM	[48]
Carbamazepine	1, 2, 5 mM	5 mM	[50]
Carbamazepine	0.5, 1, 5, 10, 50, 100, 150 mM	100 mM	[51]
Carbamazepine	0.5, 1, 2, 4, 8 mM	2 mM	[39]
Dinitrotoluenes	25.9, 37, 48.1, 63 mM	63 mM	[54]
Dinitrotoluenes	84, 105, 126, 147 mM	126 mM	[96]
Diuron	0.1, 0.25, 0.5, 0.75, 1 mM	1 mM	[40]
Greywater	3, 4.5, 6, 7.5, 9 mM	9 mM	[97]
Hexachlorocyclohexanes	0.5, 1, 2, 4 mM	2 mM	[84]
Methyl orange	4, 6, 8, 10, 20 mM	10 mM	[69]
Orange II	4.2, 6.3, 8.4, 12.6, 16.8 mM	16.8 mM	[28]
Orange II	4.2, 8.4, 16.8 mM	8.4 mM	[85]
Orange G	0.05, 0.5, 1, 5 mM	5 mM	[66]
Oxcarbazepine	0.1, 0.25, 0.5, 0.75, 1 mM	1 mM	[30]
Pentachlorophenol	33, 49, 69, 82, 99, 115 μM	115 μM	[87]
Ponceau 6R	1, 1.5, 2, 3, 4 mM	4 mM	[95]
Pulp and paper wastewater	2, 4, 6, 8 mM	6 mM	[98]
Reactive Brilliant Blue	1, 4, 5, 10 mM	10 mM	[88]
Sodium dodecylbenzene sulfonate	10, 25, 50, 100 mM	25 mM	[68]
Sulfamethoxazole	0.1, 1, 2, 5 mM	5 mM	[56]
Tetracycline hydrochloride	4.2, 8.4, 12.6, 16.8 mM	12.6 mM	[57]
Toluene	10, 20, 30 mM	30 mM	[59]

3.6. Temperature

Temperature is an important parameter for the solution viscosity [99] and mass transfer coefficients [100]. As a result, temperature is frequently considered due to its crucial influence on the degradation of organic contaminants in EPOPs [43,44]. It was observed that the degradation efficiency of TOC (aniline solution) at 318 K was higher than that at 313 K during the electro-activated persulfate process, indicating that a higher reaction temperature was beneficial to the mineralization of aniline [43]. A similar phenomenon was also found in other studies using EPOPs, including the treatments of Disperse Blue

3 [83], carbamazepine [39,51], phenol [61], landfill leachate [93], and petrochemical wastewater [94]. The enhancement of the degradation efficiency with an increase in temperature could be ascribed to multiple mechanisms. Firstly, an increase in temperature is beneficial for mass transfer in the reaction system [61], which would accelerate the reaction process. Secondly, heat can activate PS, promoting the generation of $SO_4^{\bullet-}$ [101]. Finally, the amount of oxygen gas dissolved in wastewater would decrease at higher reaction temperatures, which could facilitate the contact between the persulfate anions and cathode and lead to the formation of sulfate radicals [43,44]. Nevertheless, it was still found that a continued increase in temperature did not promote the removal of organic contaminants in several studies [76,79]. The negative influence of extremely high temperatures could be attributed to some quenching reactions (Equations (13) and (15)) [76].

3.7. Nitrogen/Oxygen Dosage

Nitrogen and oxygen dosages also affect the generation of sulfate radicals during the electro-activated persulfate process [43,44,54]. The influence of the flow rate of nitrogen and oxygen on the electrolytic behavior has been investigated in the degradation of dinitrotoluenes, aniline [43,44], and Disperse Blue 3 [83]. It was found that the TOC removal efficiency of industrial wastewater containing dinitrotoluenes increased with the increase in nitrogen dosage [54]. In contrast, the degradation efficiency of TOC decreased upon raising the oxygen flow rate [54]. Similarly, under O_2-saturated conditions, a considerable amount of H_2O_2 was generated, leading to lower PS decomposition and 25% less decolorization of Disperse Blue 3 compared to the control reaction [83]. However, under N_2-saturated conditions, an effective decolorization of about 99% was achieved [83]. The phenomenon may be attributed to nitrogen enhancement in the amounts of sulfate radicals generated via the cathodic reduction of persulfate anions, which would compete with oxygen for electrons (Equations (16) and (17)) [44]. Upon introduction of nitrogen gas, the oxygen formed from anodic oxidation of water would be expelled from the wastewater, resulting in the production of a lower amount of H_2O_2 [54]. Conversely, there was an increase in the number of dissolved oxygen molecules, which intensely competed with persulfate anions for electrons at the cathode and then inhibited the PS activation process [43].

$$S_2O_8^{2-} + e^- \rightarrow SO_4^{\bullet-} + SO_4^{2-} \tag{16}$$

$$O_2 + 2H^+ + 2e^- \rightarrow H_2O_2 \tag{17}$$
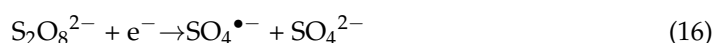
3.8. Coexisting Ions and Natural Organic Matter

The effects of coexisting inorganic anions on the degradation efficiency of EPOPs have been well studied due to their ubiquitous distribution in various types of water [40,41,50]. The effects of Cl^-, HCO_3^-, CO_3^{2-}, NO_3^-, SO_4^{2-}, and $H_2PO_4^-$ have been mentioned in previous studies [31,40,50]. Generally, these inorganic anions have negative effects on sulfate and hydroxyl radicals because these ions can quench the sulfate and hydroxyl radicals via Equations (18)–(27) [31,40,50]. Less-reactive inorganic radical species are generated after these reactions, causing lower degradation efficiencies of the organic contaminants. Nevertheless, Cl^- was found to promote the degradation of target organic contaminants in some studies using EPOPs [31,41,50,80]. Ma et al. [41] found that low concentrations of Cl^- inhibited the degradation of 2,4-dinitrotoluene in the earlier part of the reaction, whereas high concentrations of Cl^- facilitated the degradation of 2,4-dinitrotoluene. Similarly, it was reported that Cl^- enhanced the decomposition of carbamazepine in electrochemically activated PS oxidation [50]. The influence of Cl^- on degradation might change along with the structure of the pollutants [11]. If chlorine radicals (e.g., $Cl^\bullet$ and $Cl_2^{\bullet-}$) are effective for organic contaminants with certain molecular structures, then the enhanced generation of chlorine radicals (e.g., $Cl^\bullet$ and $Cl_2^{\bullet-}$) using electrochemistry could promote the degradation efficiencies in these studies. It was reported that the presence of Cl^- accelerated the degradation of ATZ, with the rate constant increasing from 0.050 to 0.069 min^{-1}. As for SO_4^{2-}, it is the byproduct of PS activation reactions. Although it cannot be easily oxidized,

$S_2O_8{}^{2-}$ can be generated from $SO_4{}^{2-}$ via Equation (6), which could be considered as an effective supply of PS [25]. Meanwhile, sulfate ions could act as an electrolyte to improve the reactions.

$$SO_4{}^{\bullet-} + Cl^- \rightarrow SO_4{}^{2-} + Cl^\bullet \tag{18}$$

$$^\bullet OH + Cl^- \rightarrow OH^- + Cl^\bullet \tag{19}$$

$$Cl^- + Cl^\bullet \rightarrow Cl_2{}^{\bullet-} \tag{20}$$

$$SO_4{}^{\bullet-} + HCO_3{}^- \rightarrow SO_4{}^{2-} + H^+ + CO_3{}^{\bullet-} \tag{21}$$

$$SO_4{}^{\bullet-} + CO_3{}^{2-} \rightarrow SO_4{}^{2-} + CO_3{}^{\bullet-} \tag{22}$$

$$^\bullet OH + HCO_3{}^- \rightarrow H_2O + CO_3{}^{\bullet-} \tag{23}$$

$$^\bullet OH + CO_3{}^{2-} \rightarrow OH^- + CO_3{}^{\bullet-} \tag{24}$$

$$SO_4{}^{\bullet-} + NO_3{}^- \rightarrow SO_4{}^{2-} + NO_3{}^\bullet \tag{25}$$

$$^\bullet OH + NO_3{}^- \rightarrow NO_3{}^\bullet + OH^- \tag{26}$$

$$SO_4{}^{\bullet-} + H_2PO_4{}^- \rightarrow H_2PO_4{}^\bullet + SO_4{}^{2-} \tag{27}$$
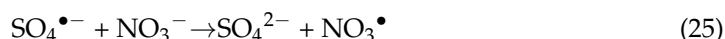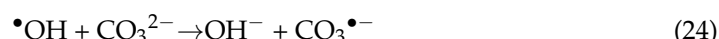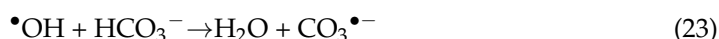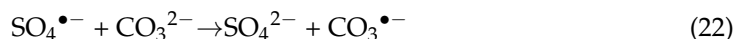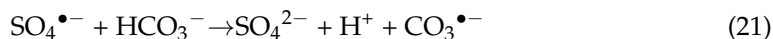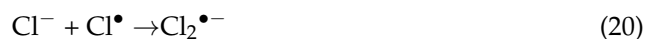
Natural organic matter (NOM) is able to scavenge radicals, which can lower the degradation efficiency [50]. It is necessary to investigate the effects of NOM on the degradation of target compounds in EPOPs. Suwannee River natural organic matter [30] and humic acid [50,70] have been used as representative NOM to simulate the coexisting process. Bu et al. [30] found that the degradation rate of oxcarbazepine decreased from 0.14 min^{-1} to 0.05 min^{-1} when the dosage of NOM increased from 0 mg/L to 10 mg/L. The rapidly decreasing pseudo-first-order rate constant of oxcarbazepine degradation at low dosages of NOM can be ascribed to the sharp consumption of $^\bullet OH$ by NOM based on the reaction rate constants [30]. Similarly, the addition of humic acid during electrochemically activated PS oxidation significantly inhibited the decomposition of carbamazepine [50]. The phenomenon could be ascribed to the reasons involved in competitive contact and oxidation [50]. Therefore, it can be deduced that competitive contact and oxidation are the predominant mechanisms of NOM inhibition.

4. Degradation Mechanisms

The removal mechanisms of EPOPs are mainly considered to be the joint contributions of the radical-induced reactions [82] and non-radical oxidation [50] (Figure 2). Radical-induced reactions, typically involving $SO_4{}^{\bullet-}$ and $^\bullet OH$, have been frequently reported [82,83]. The predominant radical reactions are listed in Table 5. Around the cathode, $SO_4{}^{\bullet-}$ can be generated from $S_2O_8{}^{2-}$ via a cathodic activation, which is the chief source of $SO_4{}^{\bullet-}$ in EPOPs [82]. Under O_2-saturated conditions, a considerable amount of H_2O_2 was generated via Equation (17), leading to a lower PS decomposition [83]. It was found that the number of oxygen molecules dissolved in the electrolyte increased, which intensely competed with persulfate anions for electrons at the cathode and then inhibited the PS activation process [43]. Although the generated H_2O_2 could be converted to $^\bullet OH$, its standard redox potential is lower than that of $SO_4{}^{\bullet-}$ [2]. Around the anode, a certain amount of hydroxyl radicals (M($^\bullet OH$)) are formed as an intermediate of water discharge on the anode (M) [102], which is the original reason for anode oxidation. In addition, oxidants can be generated from $SO_4{}^{2-}$, as reported in some previous studies [25,27,71]. On the one hand, $S_2O_8{}^{2-}$ can be generated from $SO_4{}^{2-}$ via Equation (6), which could be considered as an effective supply of PS [25]. Other activation methods could not regenerate PS based on a literature analysis [2]. On the other hand, it was found that $SO_4{}^{\bullet-}$ could be formed anodically from $SO_4{}^{2-}$ using BDD electrodes [71]. These results indicate that anodic reactions also contribute to the degradation process, probably due to the oxidant and radical supply. It is worth mentioning that some reactions among radicals occur in EPOPs. For example, $SO_4{}^{\bullet-}$ can be converted to $^\bullet OH$ via the reaction with OH^-/H_2O [51].

Additionally, the recombination of $SO_4^{\bullet-}$ and $^{\bullet}OH$ occurs when the radical concentrations reach a certain level [51,103].
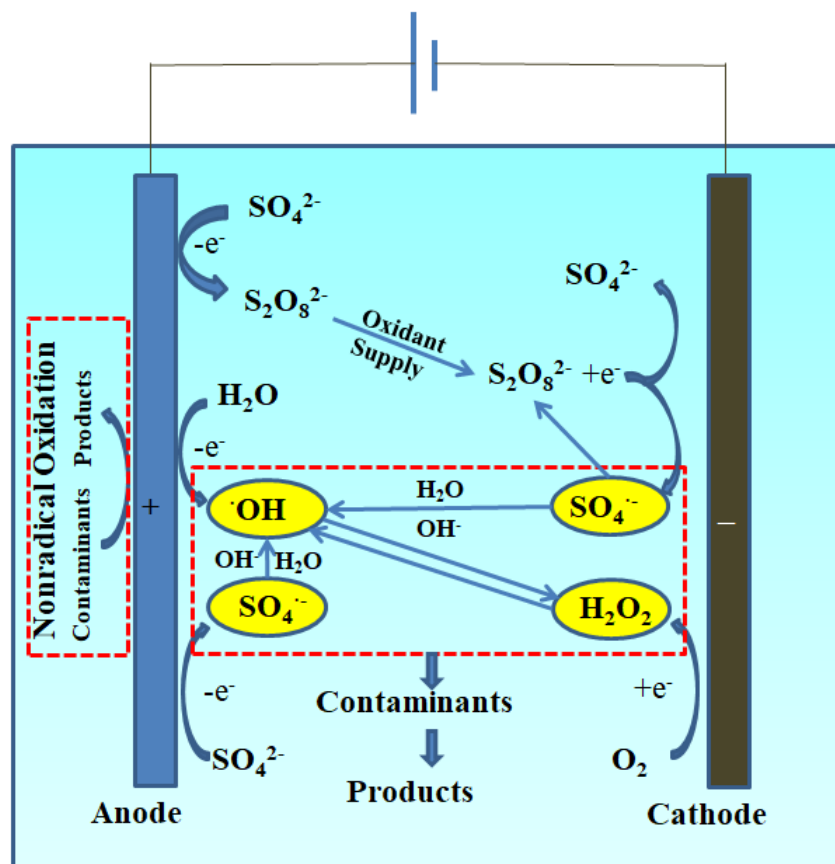
Figure 2. Possible mechanism for the removal of organic contaminants using EPOPs.

Table 5. The predominant radical reactions in EPOPs.

Reactions	Ref.
Anode:	
$M + H_2O \rightarrow M(^{\bullet}OH) + H^+ + e^-$	[74]
$2SO_4^{2-} \rightarrow S_2O_8^{2-} + 2e^-$	[25]
$SO_4^{2-} \rightarrow SO_4^{\bullet-} + e^-$	[71]
Cathode:	
$S_2O_8^{2-} + e^- \rightarrow SO_4^{\bullet-} + SO_4^{2-}$	[82]
$O_2 + 2H^+ + 2e^- \rightarrow H_2O_2$	[51]
$H_2O_2 \rightarrow 2^{\bullet}OH$	[103]
Radicals:	
$SO_4^{\bullet-} + H_2O \rightarrow H^+ + SO_4^{2-} + {}^{\bullet}OH$	[51]
$SO_4^{\bullet-} + OH^- \rightarrow SO_4^{2-} + {}^{\bullet}OH$	[51]
$^{\bullet}OH + {}^{\bullet}OH \rightarrow H_2O_2$	[103]
$SO_4^{\bullet-} + SO_4^{\bullet-} \rightarrow S_2O_8^{2-}$	[51]

Note: M means the organic molecule.

In addition to radical oxidation, non-radical oxidation also contributes to the removal of contaminants [45,49,50,56]. It is known that methanol can scavenge both $^{\bullet}OH$ and $SO_4^{\bullet-}$, and tert-butanol can be used to scavenge $^{\bullet}OH$ [50,104]. Methanol (MeOH) was commonly employed as the scavenger of $SO_4^{\bullet-}$ (k = 2.5×10^7 M^{-1} s^{-1}) and $^{\bullet}OH$ (k = 9.7×10^8 M^{-1}s^{-1}), while tert-butyl alcohol (TBA) was applied as the scavenger for $^{\bullet}OH$ (k = 6.0×10^8 M^{-1}s^{-1}) [105]. Surprisingly, it was observed that the addition of excess methanol or tert-butanol at a dose up to 200 times the PDS concentration during the

electrochemically activated PDS process had negligible impact on the degradation of carbamazepine [50]. Similar results were reported in other studies involving the degradation of sulfamethoxazole [56] and aniline [45]. NaN_3 is usually employed for $^1O_2$ quenching [105]. Moreover, Nie et al. [45] found that the addition of NaN_3 had negligible impact on the degradation of acyclovir, indicating that singlet oxygen was not responsible for the EC activation of PDS at a multi-walled carbon nanotube (MWCNT) cathode. The above results indicate that nonradical oxidation mainly contributed to the degradation of target organic compounds. It is known that electrical discharge in an electric double layer induces the stable PDS molecule into a transition (activated) state and that the activated PDS molecule has high reactivity, which can degrade organic compounds [50]. Analogously, Nie et al. [45] suggested that the MWCNT-adsorbed $S_2O_8^{2-}$ with a modified electronic structure was highly reactive towards organic compounds. Although suitable in situ characterization methods for investigating the modified electronic structure of PDS are lacking at present [45], this explanation provides a plausible non-radical mechanism. Until now, the non-radical mechanisms have not been adequately studied. More in-depth investigations are still needed to reveal the exact non-radical mechanisms.

It is worth mentioning that various other methods have been combined with EPOPs, as demonstrated in Table 1. These methods were shown to be effective at enhancing the removal efficiencies using EPOPs (Table 1). Ultrasound and Fe^{2+}/Fe^{3+} are selected for discussion in this study. Ultrasound enhancement could be attributed to cavitation, PS activation, and mass transfer intensification [2]. The decolorization efficiency of Acid Orange 7 increased with the increase in Fe^{2+} concentration due to the PS activation of the available Fe^{2+} [23]. Therefore, more $SO_4^{\bullet-}$ are generated to oxidate bisphenol A with Fe^{2+} involvement [29]. In addition, some heterogeneous catalysts (e.g., Fe/SBA-15 [85], MnO_2 [42]) were used to promote the removal efficiencies. These combination methods also play important roles in the degradation of organic contaminants using EPOPS.

5. Energy Consumption and Limitations

5.1. Energy Consumption

Energy consumption is a key point in evaluating a method of organic contaminant treatment, especially for field applications [76]. Although no cost comparison has been made among various PS activation methods, there are several studies involving the energy consumption of EPOPs in the past decade (Table 6). It can be seen that the electrical energy consumption of EPOPs has been controlled at a reasonably low range, which is undoubtedly favorable for further field applications. Cai et al. [85] found that the electrical energy consumption per order of magnitude (EE/O) of the EC/Fe/SBA-15/PDS process was 9.87 kWh/m^3, which was much lower compared to $UV/ZnO/H_2O_2$ (172 kWh/m^3) [103] and $UV/[TiO_2 + ZnO]/PDS$ (18.08 kWh/m^3) [106]. Similarly, the removal rate of Acid Orange 7 reached 98.1% at 30 min in the electro/MnO_2/PDS system; the EE/O of the oxidation system was 7.84 kWh/m^3, which was much smaller than some photocatalysis processes [42]. In addition, the EE/O of sulfamethoxazole degradation efficiency using the EC/PDS process was calculated to be only 0.04 kWh/m^3 under optimal conditions [89]. It was reported that the EE/O value for sulfamethoxazole removal was 0.46 kWh/m^3 for an electron beam, 27.53 kWh/m^3 for ozone oxidation, 1.50 kWh/m^3 for UV-C photodegradation, and 13.2–21.6 kWh/m^3 for electrochemical degradation using a Ti/SnO_2-Sb/Ce-PbO_2 anode [89,107,108]. Apart from the comparison with other methods, the electrode material [39] and catalyst assistance [78] are also crucial for cost reduction in EPOPs. When a Pt cathode was replaced with activated carbon fiber, the EE/O value decreased from 0.6056 kWh/m^3 to 0.0788 kWh/m^3 in the EC/Fe^{3+}/PDS system [39]. It was reported that the electrical energy consumption decreased from 1.151 kWh/g to 0.744 kWh/g with the addition of a nano-Fe@NdFeB/AC catalyst [78]. Overall, electrolysis assisted persulfate oxidation is an energy-saving method for removing some organic contaminants with the appropriate operational conditions.

Table 6. The energy consumption of EPOPs in previous studies.

System	Analytes	$C_{initial}$	Electricity Energy Consumption (kWh/m^3)	Ref.
EC/Pyrite/PMS	1-Butyl-1-methylpyrrolidinium chloride	323.43 mg/L	5.45 kWh/m^3	[77]
EC/AIS/PDS	2, 4-Dinitrophenol	200 mg/L	0.0336 kWh/m^3	[79]
EC/Nano-Fe@NdFeB/AC/PDS	2,4,6-Trichlorophenol	10 mg/L	7.44 kWh/m^3 (TOC)	[78]
EC/MnO$_2$/PDS	Acid Orange 7	49 mg/L	7.84 kWh/m^3	[42]
EC/Fe$_3$O$_4$/PDS	Acid Orange 7	25 mg/L	8.64 kWh/m^3	[102]
EC/CuFe$_2$O$_4$/PDS	Atrazine	9.92 mg/L	0.21 kWh/g	[80]
EC/Fe^{3+}/PDS	Carbamazepine	9.45 mg/L	0.0788 kWh/m^3	[39]
EC/Fe/SBA-15/PDS	Orange II	105.1 mg/L	9.87 kWh/m^3	[85]
EC/PDS	Sulfamethoxazole	25.33 mg/L	0.04 kWh/m^3	[89]
EC/PDS	Tetracycline hydrochloride	50 mg/L	11.48 kWh/m^3	[57]

Note: AIS: Annular iron sheet; Nano-Fe@NdFeB: Iron boron/activated carbon nanocomposite; SBA: 15-Mesoporous silica.

5.2. Limitations

There are still several limitations for the further application of EPOPs. To the best of our knowledge, the following drawbacks should be noted and considered in the future:

(1) Most EPOPs perform well in acidic conditions. A pH adjustment for efficient pollutant removal can contribute to the operational cost of EPOPs.

(2) A lower performance in aerated conditions is usually found in practical applications.

(3) Potential electrode fouling needs to be eliminated in time. The electrode performance should be effectively monitored.

(4) The concentration of sulfate ions inevitably increases during PS activation processes. The introduction of sulfate ions into the effluent should be considered later.

(5) The formation of hydrated iron hydroxide/oxide film on the surface of an iron anode reduces the effective current transfer between the anode and cathode. Acidic reaction conditions could avoid the occurrence of this phenomenon.

6. Summary and Conclusions

The combination between electrochemistry and persulfate as electrochemically assisted persulfate oxidation processes (EPOPs) is a promising substitution for traditional advanced oxidation processes. In this review, the synergistic effects of electrochemistry and persulfate, the operational variables influencing the removal efficiency, the predominant degradation mechanisms, and energy consumption were discussed and summarized. The effects of operational variables on the removal efficiency, including the electrode material, electrolyte type and concentration, current density, pH, PS concentration, temperature, nitrogen/oxygen dosage, coexisting ions, and natural organic matter, were discussed to provide beneficial references for further research. A comparison among these variables revealed that EPOPs are complicated and target depended. In addition, it was found that the decomposition mechanisms of EPOPs mainly involved the combined contributions of radical-induced reactions and non-radical oxidation. $SO_4^{\bullet-}$ and $^{\bullet}OH$ are the dominant reactive radicals in the radical-induced reactions. The regeneration of oxidants (including $S_2O_8^{2-}$ and $SO_4^{\bullet-}$) around the anode is favorable for the economic feasibility of EPOPs. Non-radical oxidation also contributes to the degradation of target compounds, while the mechanism should be further explored. The transition (activated) state of PS has high reactivity and is believed to be responsible for non-radical oxidation in EPOPs. The energy consumption estimation indicates that electrolysis-assisted persulfate oxidation is

an energy-saving method for removing some organic contaminants with the appropriate operational conditions. Nonetheless, there are still several gaps in our knowledge and limitations that require further exploration, including a lack of in situ applications, lower performance in aerated conditions, unclear mechanisms of non-radical oxidation, and few toxicity evaluations of intermediate products. In the future, more actual applications of EPOPs need to be conducted for complicated real waters with trace concentrations of organic contaminants.

Author Contributions: Conceptualization, J.S. and L.Y.; methodology, J.S.; formal analysis, W.Z. and G.H.; investigation, F.L. and S.L.; data curation, W.Z.; writing—original draft preparation, J.S.; writing—review and editing, L.Y. and Z.Z.; supervision, L.Y.; project administration, L.Y.; funding acquisition, Z.Z. All authors have read and agreed to the published version of the manuscript.

Data Availability Statement: Not applicable.

Conflicts of Interest: The authors declare no conflict of interest.

References

1. Devi, P.; Das, U.; Dalai, A.K. In-situ chemical oxidation: Principle and applications of peroxide and persulfate treatments in wastewater systems. *Sci. Total Environ.* **2016**, *571*, 643–657. [CrossRef] [PubMed]
2. Yang, L.; Xue, J.; He, L.; Wu, L.; Ma, Y.; Chen, H.; Li, H.; Peng, P.; Zhang, Z. Review on ultrasound assisted persulfate degradation of organic contaminants in wastewater: Influences, mechanisms and prospective. *Chem. Eng. J.* **2019**, *378*, 122146. [CrossRef]
3. Wacławek, S.; Lutze, H.V.; Grübel, K.; Padil, V.V.T.; Černík, M.; Dionysiou, D.D. Chemistry of persulfates in water and wastewater treatment: A review. *Chem. Eng. J.* **2017**, *330*, 44–62. [CrossRef]
4. Wang, J.; Wang, S. Activation of persulfate (PS) and peroxymonosulfate (PMS) and application for the degradation of emerging contaminants. *Chem. Eng. J.* **2018**, *334*, 1502–1517.
5. Nzeribe, B.N.; Crimi, M.; Mededovic Thagard, S.; Holsen, T.M. Physico-Chemical Processes for the Treatment of Per- And Polyfluoroalkyl Substances (PFAS): A review. *Crit. Rev. Environ. Sci. Technol.* **2019**, *49*, 866–915. [CrossRef]
6. Guerra-Rodríguez, S.; Rodríguez, E.; Singh, D.N.; Rodríguez-Chueca, J. Assessment of Sulfate Radical-Based Advanced Oxidation Processes for Water and Wastewater Treatment: A Review. *Water* **2018**, *10*, 1828.
7. Wang, S.; Zhou, N.; Wu, S.; Zhang, Q.; Yang, Z. Modeling the oxidation kinetics of sono-activated persulfate's process on the degradation of humic acid. *Ultrason. Sonochem.* **2015**, *23*, 128–134. [CrossRef]
8. Tan, C.; Gao, N.; Deng, Y.; An, N.; Deng, J. Heat-activated persulfate oxidation of diuron in water. *Chem. Eng. J.* **2012**, *203*, 294–300. [CrossRef]
9. Bruton, T.A.; Sedlak, D.L. Treatment of perfluoroalkyl acids by heat-activated persulfate under conditions representative of in situ chemical oxidation. *Chemosphere* **2018**, *206*, 457–464. [CrossRef]
10. Pourehie, O.; Saien, J. Treatment of real petroleum refinery wastewater with alternative ferrous-assisted UV/persulfate homogeneous processes. *Desalin. Water Treat.* **2019**, *142*, 140–147.
11. Ma, H.; Zhang, L.; Huang, X.; Ding, W.; Jin, H.; Li, Z.; Cheng, S.; Zheng, L. A novel three-dimensional galvanic cell enhanced Fe^{2+}/persulfate system: High efficiency, mechanism and damaging effect of antibiotic resistant *E. coli* and genes. *Chem. Eng. J.* **2019**, *362*, 667–678. [CrossRef]
12. Qi, C.; Liu, X.; Lin, C.; Zhang, X.; Ma, J.; Tan, H.; Ye, W. Degradation of sulfamethoxazole by microwave-activated persulfate: Kinetics, mechanism and acute toxicity. *Chem. Eng. J.* **2014**, *249*, 6–14. [CrossRef]
13. Xiao, R.; Luo, Z.; Wei, Z.; Luo, S.; Spinney, R.; Yang, W.; Dionysiou, D.D. Activation of peroxymonosulfate/persulfate by nanomaterials for sulfate radical-based advanced oxidation technologies. *Curr. Opin. Chem. Eng.* **2018**, *19*, 51–58. [CrossRef]
14. Liu, H.; Bruton, T.A.; Li, W.; Buren, J.V.; Prasse, C.; Doyle, F.M.; Sedlak, D.L. Oxidation of Benzene by Persulfate in the Presence of Fe(III)- and Mn(IV)-Containing Oxides: Stoichiometric Efficiency and Transformation Products. *Environ. Sci. Technol.* **2016**, *50*, 890–898. [CrossRef]
15. Kattel, E.; Dulova, N.; Viisimaa, M.; Tenno, T.; Trapido, M. Treatment of high-strength wastewater by Fe2+-activated persulphate and hydrogen peroxide. *Environ. Technol.* **2016**, *37*, 352–359. [CrossRef]
16. Wang, J.; Liao, Z.; Ifthikar, J.; Shi, L.; Du, Y.; Zhu, J.; Xi, S.; Chen, Z.; Chen, Z. Treatment of refractory contaminants by sludge-derived biochar/persulfate system via both adsorption and advanced oxidation process. *Chemosphere* **2017**, *185*, 754–763. [CrossRef]
17. Wang, Y.; Shen, C.; Zhang, M.; Zhang, B.-T.; Yu, Y.-G. The electrochemical degradation of ciprofloxacin using a SnO_2-Sb/Ti anode: Influencing factors, reaction pathways and energy demand. *Chem. Eng. J.* **2016**, *296*, 79–89. [CrossRef]

18. Wang, C.; Yin, L.; Xu, Z.; Niu, J.; Hou, L.-A. Electrochemical degradation of enrofloxacin by lead dioxide anode: Kinetics, mechanism and toxicity evaluation. *Chem. Eng. J.* **2017**, *326*, 911–920. [CrossRef]

19. Zhuo, Q.; Wang, J.; Niu, J.; Yang, B.; Yang, Y. Electrochemical oxidation of perfluorooctane sulfonate (PFOS) substitute by modified boron doped diamond (BDD) anodes. *Chem. Eng. J.* **2020**, *379*, 122280. [CrossRef]

20. Babuponnusami, A.; Muthukumar, K. Advanced oxidation of phenol: A comparison between Fenton, electro-Fenton, sono-electro-Fenton and photo-electro-Fenton processes. *Chem. Eng. J.* **2012**, *183*, 1–9. [CrossRef]

21. Rodrigues, A.S.; Souiad, F.; Fernandes, A.; Baía, A.; Pacheco, M.J.; Ciríaco, L.; Bendaoud-Boulahlib, Y.; Lopes, A. Treatment of fruit processing wastewater by electrochemical and activated persulfate processes: Toxicological and energetic evaluation. *Environ. Res.* **2022**, *209*, 112868. [CrossRef] [PubMed]

22. Zhao, Q.; Mao, Q.; Zhou, Y.; Wei, J.; Liu, X.; Yang, J.; Luo, L.; Zhang, J.; Chen, H.; Chen, H.; et al. Metal-free carbon materials-catalyzed sulfate radical-based advanced oxidation processes: A review on heterogeneous catalysts and applications. *Chemosphere* **2017**, *189*, 224–238. [CrossRef]

23. Wu, J.; Zhang, H.; Qiu, J. Degradation of Acid Orange 7 in aqueous solution by a novel electro/Fe^{2+}/peroxydisulfate process. *J. Hazard Mater.* **2012**, *215–216*, 138–145. [CrossRef] [PubMed]

24. Armstrong, D.A.; Huie, R.E.; Koppenol, W.H.; Lymar, S.V.; Merenyi, G.; Neta, P.; Ruscic, B.; Stanbury, D.M.; Steenken, S.; Wardman, P. Standard electrode potentials involving radicals in aqueous solution: Inorganic radicals (IUPAC Technical Report). *Pure Appl. Chem.* **2015**, *87*, 1139–1150. [CrossRef]

25. de Araújo, F.K.C.; de Barreto, P.J.P.; Cardozo, J.C.; dos Santos, E.V.; de Araújo, D.M.; Martínez-Huitle, C.A. Sulfate pollution: Evidence for electrochemical production of persulfate by oxidizing sulfate released by the surfactant sodium dodecyl sulfate. *Environ. Chem. Lett.* **2018**, *16*, 647–652. [CrossRef]

26. Yang, S.-Q.; Cui, Y.-H.; Liu, Y.-Y.; Liu, Z.-Q.; Li, X.-Y. Electrochemical generation of persulfate and its performance on 4-bromophenol treatment. *Sep. Purif. Technol.* **2018**, *207*, 461–469. [CrossRef]

27. Si, F.; Zhang, Y.; Yao, C.; Du, M.; Hussain, I.; Huang, S.; Wen, W.; Hu, X. Degradation of ronidazole by electrochemically simultaneously generated persulfate and ferrous ions. *Chemosphere* **2020**, *238*, 124579. [CrossRef]

28. Cai, C.; Zhang, H.; Zhong, X.; Hou, L. Electrochemical enhanced heterogeneous activation of peroxydisulfate by Fe–Co/SBA-15 catalyst for the degradation of Orange II in water. *Water Res.* **2014**, *66*, 473–485. [CrossRef]

29. Lin, H.; Wu, J.; Zhang, H. Degradation of bisphenol A in aqueous solution by a novel electro/Fe3+/peroxydisulfate process. *Sep. Purif. Technol.* **2013**, *117*, 18–23. [CrossRef]

30. Bu, L.; Zhou, S.; Shi, Z.; Bi, C.; Zhu, S.; Gao, N. Iron electrode as efficient persulfate activator for oxcarbazepine degradation: Performance, mechanism, and kinetic modeling. *Sep. Purif. Technol.* **2017**, *178*, 66–74. [CrossRef]

31. Bu, L.; Zhu, S.; Zhou, S. Degradation of atrazine by electrochemically activated persulfate using BDD anode: Role of radicals and influencing factors. *Chemosphere* **2018**, *195*, 236–244. [CrossRef] [PubMed]

32. Poza-Nogueiras, V.; Rosales, E.; Pazos, M.; Sanromán, M.Á. Current advances and trends in electro-Fenton process using heterogeneous catalysts—A review. *Chemosphere* **2018**, *201*, 399–416. [CrossRef]

33. Nidheesh, P.V.; Zhou, M.; Oturan, M.A. An overview on the removal of synthetic dyes from water by electrochemical advanced oxidation processes. *Chemosphere* **2018**, *197*, 210–227. [CrossRef] [PubMed]

34. Sirés, I.; Brillas, E.; Oturan, M.A.; Rodrigo, M.A.; Panizza, M. Electrochemical advanced oxidation processes: Today and tomorrow. A review. *Environ. Sci. Pollut. Res.* **2014**, *21*, 8336–8367. [CrossRef]

35. Moreira, F.C.; Boaventura, R.A.R.; Brillas, E.; Vilar, V.J.P. Electrochemical advanced oxidation processes: A review on their application to synthetic and real wastewaters. *Appl. Catal. B Environ.* **2017**, *202*, 217–261. [CrossRef]

36. Li, J.; Li, Y.; Xiong, Z.; Yao, G.; Lai, B. The electrochemical advanced oxidation processes coupling of oxidants for organic pollutants degradation: A mini-review. *Chin. Chem. Lett.* **2019**, *30*, 2139–2146. [CrossRef]

37. Anglada, Á.; Urtiaga, A.; Ortiz, I. Contributions of electrochemical oxidation to waste-water treatment: Fundamentals and review of applications. *J. Chem. Technol. Biotechnol.* **2009**, *84*, 1747–1755. [CrossRef]

38. Yu, X.; Zhou, M.; Hu, Y.; Groenen Serrano, K.; Yu, F. Recent updates on electrochemical degradation of bio-refractory organic pollutants using BDD anode: A mini review. *Environ. Sci. Pollut. Res.* **2014**, *21*, 8417–8431. [CrossRef]

39. Han, S.; Hassan, S.U.; Zhu, Y.; Zhang, S.; Liu, H.; Zhang, S.; Li, J.; Wang, Z.; Zhao, C. Significance of activated carbon fiber as cathode in electro/Fe^{3+}/peroxydisulfate oxidation process for removing carbamazepine in aqueous environment. *Ind. Eng. Chem. Res.* **2019**, *58*, 19709–19718. [CrossRef]

40. Yu, Y.; Zhou, S.; Bu, L.; Shi, Z.; Zhu, S. Degradation of Diuron by Electrochemically Activated Persulfate. *Water Air Soil Pollut.* **2016**, *227*, 279. [CrossRef]

41. Ma, Z.; Yang, Y.; Jiang, Y.; Xi, B.; Yang, T.; Peng, X.; Lian, X.; Yan, K.; Liu, H. Enhanced degradation of 2,4-dinitrotoluene in groundwater by persulfate activated using iron–carbon micro-electrolysis. *Chem. Eng. J.* **2017**, *311*, 183–190. [CrossRef]

42. Xu, Y.; Lin, H.; Li, Y.; Zhang, H. The mechanism and efficiency of MnO$_2$ activated persulfate process coupled with electrolysis. *Sci. Total Environ.* **2017**, *609*, 644–654. [CrossRef]

43. Chen, W.-S.; Huang, C.-P. Mineralization of aniline in aqueous solution by electrochemical activation of persulfate. *Chemosphere* **2015**, *125*, 175–181. [CrossRef]

44. Chen, W.-S.; Huang, C.-P. Mineralization of aniline in aqueous solution by electro-activated persulfate oxidation enhanced with ultrasound. *Chem. Eng. J.* **2015**, *266*, 279–288. [CrossRef]

45. Nie, C.; Ao, Z.; Duan, X.; Wang, C.; Wang, S.; An, T. Degradation of aniline by electrochemical activation of peroxydisulfate at MWCNT cathode: The proofed concept of nonradical oxidation process. *Chemosphere* **2018**, *206*, 432–438. [CrossRef] [PubMed]

46. Bu, L.; Ding, J.; Zhu, N.; Kong, M.; Wu, Y.; Shi, Z.; Zhou, S.; Dionysiou, D.D. Unraveling different mechanisms of persulfate activation by graphite felt anode and cathode to destruct contaminants of emerging concern. *Appl. Catal. B Environ.* **2019**, *253*, 140–148. [CrossRef]

47. Deng, B.; Li, Y.; Tan, W.; Wang, Z.; Yu, Z.; Xing, S.; Lin, H.; Zhang, H. Degradation of bisphenol A by electro-enhanced heterogeneous activation of peroxydisulfate using Mn-Zn ferrite from spent alkaline Zn-Mn batteries. *Chemosphere* **2018**, *204*, 178–185. [CrossRef]

48. Yan, S.; Zhang, X.; Shi, Y.; Zhang, H. Natural Fe-bearing manganese ore facilitating bioelectro-activation of peroxymonosulfate for bisphenol A oxidation. *Chem. Eng. J.* **2018**, *354*, 1120–1131. [CrossRef]

49. Song, H.; Yan, L.; Jiang, J.; Ma, J.; Zhang, Z.; Zhang, J.; Liu, P.; Yang, T. Electrochemical activation of persulfates at BDD anode: Radical or nonradical oxidation? *Water Res.* **2018**, *128*, 393–401. [CrossRef]

50. Song, H.; Yan, L.; Ma, J.; Jiang, J.; Cai, G.; Zhang, W.; Zhang, Z.; Zhang, J.; Yang, T. Nonradical oxidation from electrochemical activation of peroxydisulfate at Ti/Pt anode: Efficiency, mechanism and influencing factors. *Water Res.* **2017**, *116*, 182–193. [CrossRef]

51. Liu, Z.; Zhao, C.; Wang, P.; Zheng, H.; Sun, Y.; Dionysiou, D.D. Removal of carbamazepine in water by electro-activated carbon fiber-peroxydisulfate: Comparison, optimization, recycle, and mechanism study. *Chem. Eng. J.* **2018**, *343*, 28–36. [CrossRef]

52. Malakootian, M.; Ahmadian, M. Ciprofloxacin removal by electro-activated persulfate in aqueous solution using iron electrodes. *Appl. Water Sci.* **2019**, *9*, 140. [CrossRef]

53. Malakootian, M.; Ahmadian, M. Removal of ciprofloxacin from aqueous solution by electro-activated persulfate oxidation using aluminum electrodes. *Water Sci. Technol.* **2019**, *80*, 587–596. [CrossRef]

54. Chen, W.-S.; Jhou, Y.-C.; Huang, C.-P. Mineralization of dinitrotoluenes in industrial wastewater by electro-activated persulfate oxidation. *Chem. Eng. J.* **2014**, *252*, 166–172. [CrossRef]

55. Huang, X.; An, D.; Song, J.; Gao, W.; Shen, Y. Persulfate/electrochemical/FeCl$_2$ system for the degradation of phenol adsorbed on granular activated carbon and adsorbent regeneration. *J. Clean. Prod.* **2017**, *165*, 637–644. [CrossRef]

56. Song, H.; Yan, L.; Jiang, J.; Ma, J.; Pang, S.; Zhai, X.; Zhang, W.; Li, D. Enhanced degradation of antibiotic sulfamethoxazole by electrochemical activation of PDS using carbon anodes. *Chem. Eng. J.* **2018**, *344*, 12–20. [CrossRef]

57. Liu, J.; Zhong, S.; Song, Y.; Wang, B.; Zhang, F. Degradation of tetracycline hydrochloride by electro-activated persulfate oxidation. *J. Electroanal. Chem.* **2018**, *809*, 74–79. [CrossRef]

58. Zhang, C.; Jiang, Y.; Li, Y.; Hu, Z.; Zhou, L.; Zhou, M. Three-dimensional electrochemical process for wastewater treatment: A general review. *Chem. Eng. J.* **2013**, *228*, 455–467. [CrossRef]

59. Long, A.; Zhang, H. Selective oxidative degradation of toluene for the recovery of surfactant by an electro/Fe^{2+}/persulfate process. *Environ. Sci. Pollut. Res.* **2015**, *22*, 11606–11616. [CrossRef]

60. Park, S.-M.; Lee, S.-W.; Jeon, P.-Y.; Baek, K. Iron Anode-Mediated Activation of Persulfate. *Water Air Soil Pollut.* **2016**, *227*, 462. [CrossRef]

61. Silveira, J.E.; Cardoso, T.O.; Barreto-Rodrigues, M.; Zazo, J.A.; Casas, J.A. Electro activation of persulfate using iron sheet as low-cost electrode: The role of the operating conditions. *Environ. Technol.* **2018**, *39*, 1208–1216. [CrossRef] [PubMed]

62. Yan, S.; Xiong, W.; Xing, S.; Shao, Y.; Guo, R.; Zhang, H. Oxidation of organic contaminant in a self-driven electro/natural maghemite/peroxydisulfate system: Efficiency and mechanism. *Sci. Total Environ.* **2017**, *599–600*, 1181–1190. [CrossRef] [PubMed]

63. Zhang, H.; Wang, Z.; Liu, C.; Guo, Y.; Shan, N.; Meng, C.; Sun, L. Removal of COD from landfill leachate by an electro/Fe^{2+}/peroxydisulfate process. *Chem. Eng. J.* **2014**, *250*, 76–82. [CrossRef]

64. Long, Y.; Feng, Y.; Li, X.; Suo, N.; Chen, H.; Wang, Z.; Yu, Y. Removal of diclofenac by three-dimensional electro-Fenton-persulfate (3D electro-Fenton-PS). *Chemosphere* **2019**, *219*, 1024–1031. [CrossRef]

65. Matzek, L.W.; Carter, K.E. Activated persulfate for organic chemical degradation: A review. *Chemosphere* **2016**, *151*, 178–188. [CrossRef]

66. Jeon, P.; Park, S.-M.; Baek, K. Controlled release of iron for activation of persulfate to oxidize orange G using iron anode. *Korean J. Chem. Eng.* **2017**, *34*, 1305–1309. [CrossRef]

67. Mehralipour, J.; Leili, M.; ZolghadrNasab, H.; Seyed Mohammadi, A.; Shabanlo, A. Efficiency of Electro/Fe^{2+}/Persulfate Process in Industrial Wastewater Treatment. *J. Maz. Univ. Med. Sci.* **2015**, *25*, 137–148.

68. Samarghandi, M.R.; Mehralipour, J.; Azarin, G.; Godini, K.; Shabanlo, A. Decomposition of sodium dodecylbenzene sulfonate surfactant by Electro/Fe^{2+} -activated Persulfate process from aqueous solutions. *Glob. NEST J.* **2017**, *19*, 115–121.

69. Li, P.; Liu, Z.; Wang, X.; Guo, Y.; Wang, L. Enhanced decolorization of methyl orange in aqueous solution using iron–carbon micro-electrolysis activation of sodium persulfate. *Chemosphere* **2017**, *180*, 100–107. [CrossRef]

70. Frontistis, Z.; Mantzavinos, D.; Meriç, S. Degradation of antibiotic ampicillin on boron-doped diamond anode using the combined electrochemical oxidation—Sodium persulfate process. *J. Environ. Manag.* **2018**, *223*, 878–887. [CrossRef]

71. Matzek, L.W.; Tipton, M.J.; Farmer, A.T.; Steen, A.D.; Carter, K.E. Understanding Electrochemically Activated Persulfate and Its Application to Ciprofloxacin Abatement. *Environ. Sci. Technol.* **2018**, *52*, 5875–5883. [CrossRef] [PubMed]

72. Chen, L.; Lei, C.; Li, Z.; Yang, B.; Zhang, X.; Lei, L. Electrochemical activation of sulfate by BDD anode in basic medium for efficient removal of organic pollutants. *Chemosphere* **2018**, *210*, 516–523. [CrossRef] [PubMed]

73. Cai, J.; Zhou, M.; Liu, Y.; Savall, A.; Groenen Serrano, K. Indirect electrochemical oxidation of 2,4-dichlorophenoxyacetic acid using electrochemically-generated persulfate. *Chemosphere* **2018**, *204*, 163–169. [CrossRef]

74. Farhat, A.; Keller, J.; Tait, S.; Radjenovic, J. Removal of Persistent Organic Contaminants by Electrochemically Activated Sulfate. *Environ. Sci. Technol.* **2015**, *49*, 14326–14333. [CrossRef]

75. Shin, Y.-U.; Yoo, H.-Y.; Ahn, Y.-Y.; Kim, M.S.; Lee, K.; Yu, S.; Lee, C.; Cho, K.; Kim, H.-i.; Lee, J. Electrochemical oxidation of organics in sulfate solutions on boron-doped diamond electrode: Multiple pathways for sulfate radical generation. *Appl. Catal. B Environ.* **2019**, *254*, 156–165. [CrossRef]

76. Xue, W.-J.; Cui, Y.-H.; Liu, Z.-Q.; Yang, S.-Q.; Li, J.-Y.; Guo, X.-L. Treatment of landfill leachate nanofiltration concentrate after ultrafiltration by electrochemically assisted heat activation of peroxydisulfate. *Sep. Purif. Technol.* **2020**, *231*, 115928. [CrossRef]

77. Arellano, M.; Sanromán, M.A.; Pazos, M. Electro-assisted activation of peroxymonosulfate by iron-based minerals for the degradation of 1-butyl-1-methylpyrrolidinium chloride. *Sep. Purif. Technol.* **2019**, *208*, 34–41. [CrossRef]

78. Yang, C.; Ren, B.; Wang, D.; Tang, Q. Synthesis of Nano-Fe@NdFeB/AC magnetic catalytic particle electrodes and application in the degradation of 2,4,6-trichlorophenol by electro-assisted peroxydisulfate process. *Environ. Technol.* **2019**, *41*, 2464–2477. [CrossRef]

79. Li, J.; Ren, Y.; Lai, L.; Lai, B. Electrolysis assisted persulfate with annular iron sheet as anode for the enhanced degradation of 2,4-dinitrophenol in aqueous solution. *J. Hazard Mater.* **2018**, *344*, 778–787. [CrossRef]

80. Li, J.; Yan, J.; Yao, G.; Zhang, Y.; Li, X.; Lai, B. Improving the degradation of atrazine in the three-dimensional (3D) electrochemical process using CuFe2O4 as both particle electrode and catalyst for persulfate activation. *Chem. Eng. J.* **2019**, *361*, 1317–1332. [CrossRef]

81. Gozmen, B.; Sonmez, O.; Sozutek, A. Comparative mineralization of Basic Red 18 with electrochemical advanced oxidation processes. *J. Serb. Chem. Soc.* **2018**, *83*, 93–105. [CrossRef]

82. Zeng, H.; Liu, S.; Chai, B.; Cao, D.; Wang, Y.; Zhao, X. Enhanced Photoelectrocatalytic Decomplexation of Cu–EDTA and Cu Recovery by Persulfate Activated by UV and Cathodic Reduction. *Environ. Sci. Technol.* **2016**, *50*, 6459–6466. [CrossRef] [PubMed]

83. Silveira, J.E.; Garcia-Costa, A.L.; Cardoso, T.O.; Zazo, J.A.; Casas, J.A. Indirect decolorization of azo dye Disperse Blue 3 by electro-activated persulfate. *Electrochim. Acta* **2017**, *258*, 927–932. [CrossRef]

84. Wacławek, S.; Antoš, V.; Hrabák, P.; Černík, M.; Elliott, D. Remediation of hexachlorocyclohexanes by electrochemically activated persulfates. *Environ. Sci. Pollut. Res.* **2016**, *23*, 765–773. [CrossRef]

85. Cai, C.; Zhang, Z.; Zhang, H. Electro-assisted heterogeneous activation of persulfate by Fe/SBA-15 for the degradation of Orange II. *J. Hazard Mater.* **2016**, *313*, 209–218. [CrossRef]

86. Luo, H.; Li, C.; Sun, X.; Chen, S.; Ding, B.; Yang, L. Ultraviolet assists persulfate mediated anodic oxidation of organic pollutant. *J. Electroanal. Chem.* **2017**, *799*, 393–398. [CrossRef]

87. Govindan, K.; Raja, M.; Noel, M.; James, E.J. Degradation of pentachlorophenol by hydroxyl radicals and sulfate radicals using electrochemical activation of peroxomonosulfate, peroxodisulfate and hydrogen peroxide. *J. Hazard Mater.* **2014**, *272*, 42–51. [CrossRef]

88. Li, X.; Tang, S.; Yuan, D.; Tang, J.; Zhang, C.; Li, N.; Rao, Y. Improved degradation of anthraquinone dye by electrochemical activation of PDS. *Ecotox Environ. Safe* **2019**, *177*, 77–85. [CrossRef]

89. Zhang, L.; Ding, W.; Qiu, J.; Jin, H.; Ma, H.; Li, Z.; Cang, D. Modeling and optimization study on sulfamethoxazole degradation by electrochemically activated persulfate process. *J. Clean. Prod.* **2018**, *197*, 297–305. [CrossRef]

90. Yuan, S.; Liao, P.; Alshawabkeh, A.N. Electrolytic Manipulation of Persulfate Reactivity by Iron Electrodes for Trichloroethylene Degradation in Groundwater. *Environ. Sci. Technol.* **2014**, *48*, 656–663. [CrossRef]

91. Tsitonaki, A.; Petri, B.; Crimi, M.; MosbÆK, H.; Siegrist, R.L.; Bjerg, P.L. In Situ Chemical Oxidation of Contaminated Soil and Groundwater Using Persulfate: A Review. *Crit. Rev. Environ. Sci. Technol.* **2010**, *40*, 55–91. [CrossRef]

92. Xu, X.-R.; Li, X.-Z. Degradation of azo dye Orange G in aqueous solutions by persulfate with ferrous ion. *Sep. Purif. Technol.* **2010**, *72*, 105–111. [CrossRef]

93. Silveira, J.E.; Zazo, J.A.; Casas, J.A. Coupled heat-activated persulfate—Electrolysis for the abatement of organic matter and total nitrogen from landfill leachate. *Waste Manag.* **2019**, *97*, 47–51. [CrossRef]

94. Yousefi, N.; Pourfadakari, S.; Esmaeili, S.; Babaei, A.A. Mineralization of high saline petrochemical wastewater using Sonoelectro-activated persulfate: Degradation mechanisms and reaction kinetics. *Microchem. J.* **2019**, *147*, 1075–1082. [CrossRef]

95. El-Zomrawy, A.A. Kinetic studies of photoelectrocatalytic degradation of Ponceau 6R dye with ammonium persulfate. *J. Saudi Chem. Soc.* **2013**, *17*, 397–402. [CrossRef]

96. Chen, W.-S.; Huang, C.-P. Mineralization of dinitrotoluenes in aqueous solution by sono-activated persulfate enhanced with electrolytes. *Ultrason. Sonochem.* **2019**, *51*, 129–137. [CrossRef]

97. Ahmadi, M.; Ghanbari, F. Optimizing COD removal from greywater by photoelectro-persulfate process using Box-Behnken design: Assessment of effluent quality and electrical energy consumption. *Environ. Sci. Pollut. Res.* **2016**, *23*, 19350–19361. [CrossRef]

98. Jaafarzadeh, N.; Ghanbari, F.; Alvandi, M. Integration of coagulation and electro-activated HSO_5^- to treat pulp and paper wastewater. *Sustain. Environ. Res.* **2017**, *27*, 223–229. [CrossRef]

99. Hou, L.; Wang, L.; Royer, S.; Zhang, H. Ultrasound-assisted heterogeneous Fenton-like degradation of tetracycline over a magnetite catalyst. *J. Hazard Mater.* **2016**, *302*, 458–467. [CrossRef]

100. Liu, F.Z.; Yi, P.; Wang, X.; Gao, H.; Zhang, H. Degradation of Acid Orange 7 by an ultrasound/ZnO-GAC/persulfate process. *Sep. Purif. Technol.* **2018**, *194*, 181–187. [CrossRef]
101. Duan, X.; Indrawirawan, S.; Kang, J.; Tian, W.; Zhang, H.; Duan, X.; Zhou, X.; Sun, H.; Wang, S. Synergy of carbocatalytic and heat activation of persulfate for evolution of reactive radicals toward metal-free oxidation. *Catal. Today* **2019**, *355*, 319–324. [CrossRef]
102. Lin, H.; Zhang, H.; Hou, L. Degradation of C. I. Acid Orange 7 in aqueous solution by a novel electro/Fe$_3$O$_4$/PDS process. *J. Hazard Mater.* **2014**, *276*, 182–191. [CrossRef] [PubMed]
103. Daneshvar, N.; Rasoulifard, M.H.; Khataee, A.R.; Hosseinzadeh, F. Removal of C.I. Acid Orange 7 from aqueous solution by UV irradiation in the presence of ZnO nanopowder. *J. Hazard Mater.* **2007**, *143*, 95–101. [CrossRef]
104. Buxton, G.V.; Greenstock, C.L.; Helman, W.P.; Ross, A.B. Critical Review of rate constants for reactions of hydrated electrons, hydrogen atoms and hydroxyl radicals ($\cdot$OH/$\cdot$O$-$ in Aqueous Solution. *J. Phys. Chem. Ref. Data* **1988**, *17*, 513–886. [CrossRef]
105. Shen, S.; Zhou, X.; Zhao, Q.; Jiang, W.; Wang, J.; He, L.; Ma, Y.; Yang, L.; Chen, Z. Understanding the nonradical activation of peroxymonosulfate by different crystallographic MnO$_2$: The pivotal role of MnIII content on the surface. *J. Hazard Mater.* **2022**, *439*, 129613. [CrossRef] [PubMed]
106. Sadik, W.A. Decolourization of an Azo Dye by Heterogeneous Photocatalysis. *Process Saf. Environ. Prot.* **2007**, *85*, 515–520. [CrossRef]
107. Kim, T.-H.; Kim, S.D.; Kim, H.Y.; Lim, S.J.; Lee, M.; Yu, S. Degradation and toxicity assessment of sulfamethoxazole and chlortetracycline using electron beam, ozone and UV. *J. Hazard Mater.* **2012**, *227–228*, 237–242. [CrossRef]
108. Lin, H.; Niu, J.; Xu, J.; Li, Y.; Pan, Y. Electrochemical mineralization of sulfamethoxazole by Ti/SnO$_2$-Sb/Ce-PbO$_2$ anode: Kinetics, reaction pathways, and energy cost evolution. *Electrochim. Acta* **2013**, *97*, 167–174. [CrossRef]